IMPACT OF THE 1982-3 AND 1986-7 PACIFIC SST ANOMALIES ON TIME MEAN PREDICTION WITH THE GLAS GCM.

M. J. Fennessy and J. Shukla
Center for Ocean-Land-Atmosphere Interactions
University of Maryland
College Park, MD 20742 U.S.A.

1. INTRODUCTION

A wide variety of El Niño SST anomaly studies have been performed by several GCM modeling groups in recent years, for a brief review see Fennessy and Shukla, 1988. Many of these studies were sensitivity experiments, utilizing simulations initialized from a climatological or random mean atmospheric state. A number of studies were carried out in order to determine the impact of observed Pacific SST anomalies on a model prediction initialized from and compared to the observed atmospheric state (WMO, 1986; Owen and Palmer, 1987; Tokioka et al., 1987; Shukla and Fennessy, 1988).

Shukla and Fennessy (1988) examined the effect on prediction with the GLAS GCM of the record El Niño SST anomalies of DJF 1982-3. They concluded that the 1982-3 Pacific SST anomalies had a very large positive impact on tropical prediction and a modest positive impact on extra-tropical prediction. The current study examines the impact on prediction with this same GCM of the 1986-7 Pacific SST anomalies, which were of much more typical magnitude than those in 1982-3. Results from the two years are compared to elucidate the differences in forecast impact from observed Pacific SST anomalies in different El Niño years.

2. MODEL AND EXPERIMENTS

The GLAS GCM used is global in extent with a 4° latitude by 5° longitude grid and 9 equally spaced sigma levels in the vertical. The planetary boundary layer is that of Deardorff (1972) as modified by Randall (1976). Supersaturation clouds occur at all 9 levels, while convective clouds (Arakawa, 1969) are limited to the lowest six levels. Further details of the model are given by Fennessy et al. (1985).

For each experiment year 3 60-day control simulations with monthly varying climatological boundary conditions everywhere and 3 60-day boundary simulations with identical boundary conditions everwhere except the Pacific were done. The NMC observed atmospheric initial conditions used were for 0000 UTC 15, 16, 17 December 1982 and 0000 UTC 1, 2, 3 January 1987 respectively. In the boundary simulations, the observed monthly SST anomalies obtained from the Climate Analysis Center (CAC) were added to the monthly climatological values used in the control simulations for the region of the Pacific from 40°S to 60°N. The model linearly interpolates the daily values before integration.

The observed SST anomaly for January 1983 (Fig. 1a) contains a very large warm anomaly across the central and eastern Pacific, with a maximum anomaly of over 4°C. The January 1987 SST anomaly (Fig. 1b) also contains a large region of warm water in the central and eastern Pacific, although the maximum magnitude is much less, about 1.5°C. The 1982-3 Pacific SST anomaly was of record magnitude, while that in

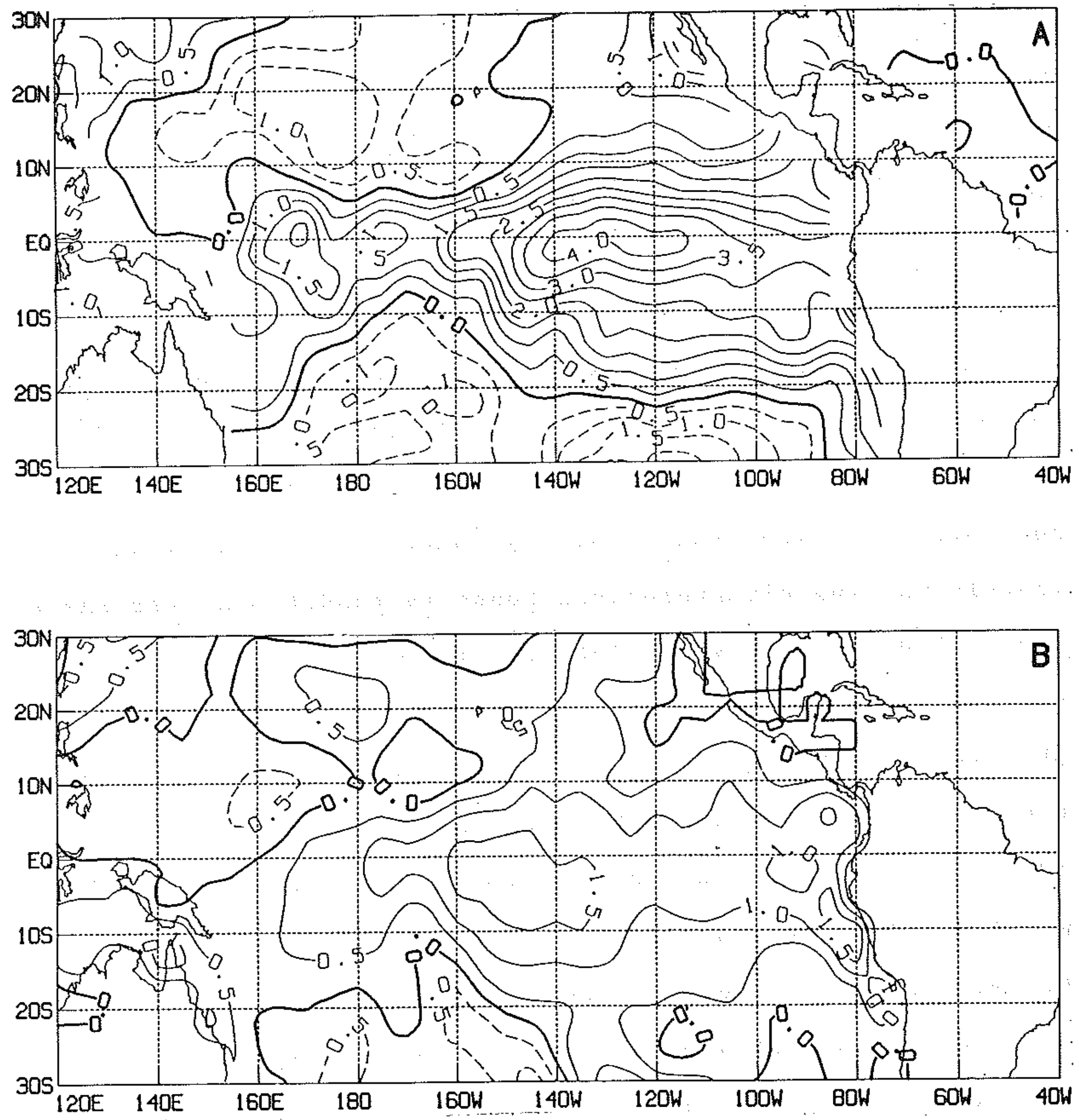

Fig. 1: January sea surface temperature anomaly for (a) 1983, and (b) 1987. Contours are 0, ± 0.5, 1, 1.5, 2, 3, and 4°C. Dashed contours are negative.

1986-7 was more typical, resembling in magnitude the composite El Niño anomaly of Rasmusson and Carpenter (1982). Thus, one might expect their impact on prediction to be quite different.

3. RESULTS

The authors have analyzed a large number of observed and simulated atmospheric fields for a wide range of time averages. From this analysis it was determined that most of the impact on prediction from the Pacific SST anomalies was on longer time scales, i.e., 30-60 days. Thus, the anomaly maps presented in this section will all be for 60-day time means. For the sake of brevity, only a few fields will be shown here. A more complete set of diagnostics for the 1982-3 experiment can be found in Shukla and Fennessy (1988).

Figures 2 and 3 depict the observed and simulated precipitation anomalies for 1982-3 and 1987, respectively. The observed precipitation anomalies (mm/day) are obtained by dividing the observed OLR anomalies (w/m^2) by -5.7, an approximate empirical relation obtained from Phil Arkin (personal communication). The model simulated anomalies depicted are simply the average of the 3 boundary integrations minus the average of the 3 control integrations for the given year. The model climate drift is automatically removed from this type of anomaly, assuming the drift is the same in control and boundary integrations. Thus, it isolates the effect of the SST anomaly. In 1982-3 a large positive anomaly (4 mm/day) was observed across the entire

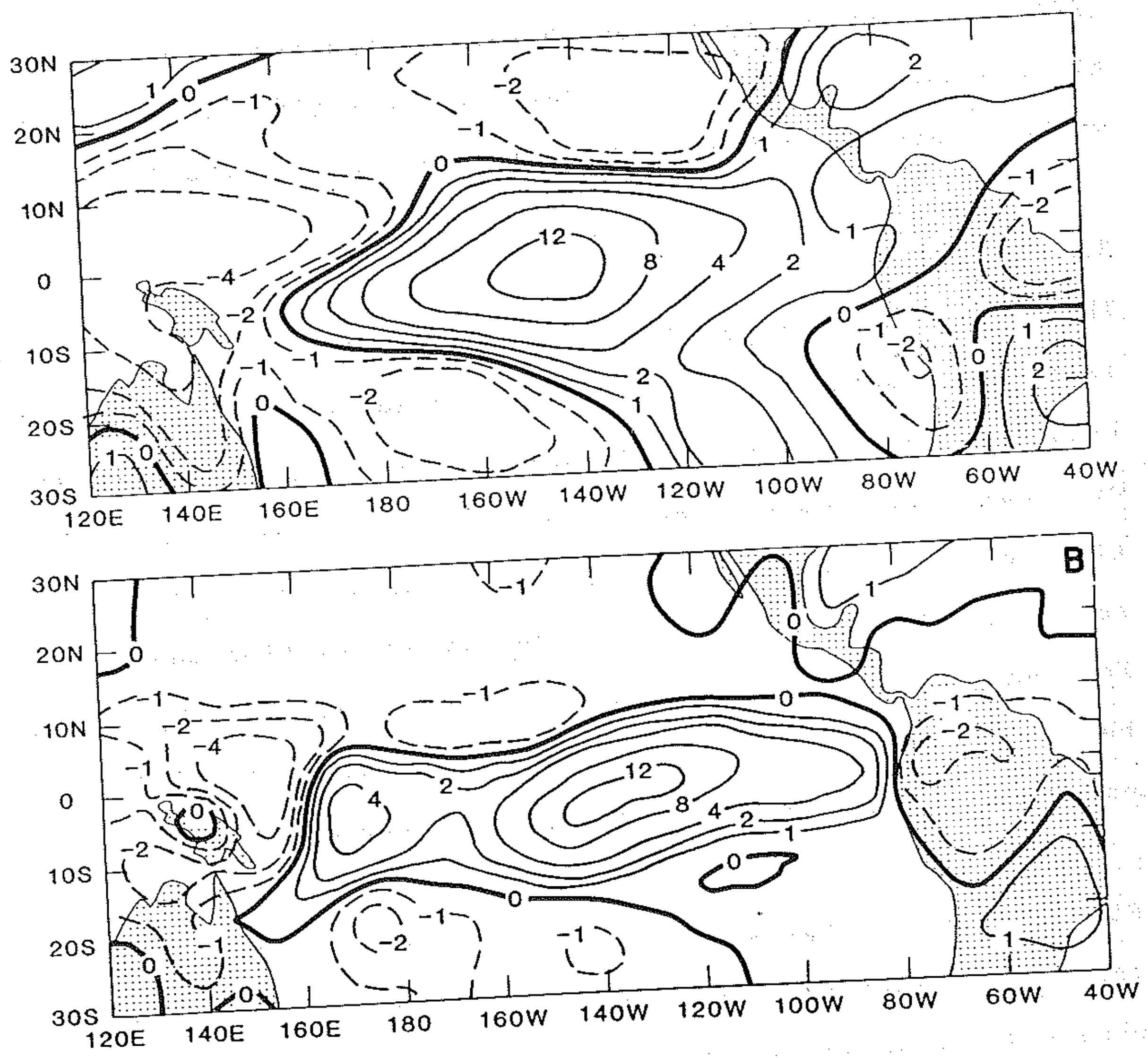

Fig. 2: 1-60 day 1982-3 mean precipitation for (a) observed anomaly calculated from observed OLR anomaly, and (b) simulated anomaly. Contours are 0, $\pm$ 1, 2, 4, 8, 12 mm day^{-1}. Dashed contours are negative.

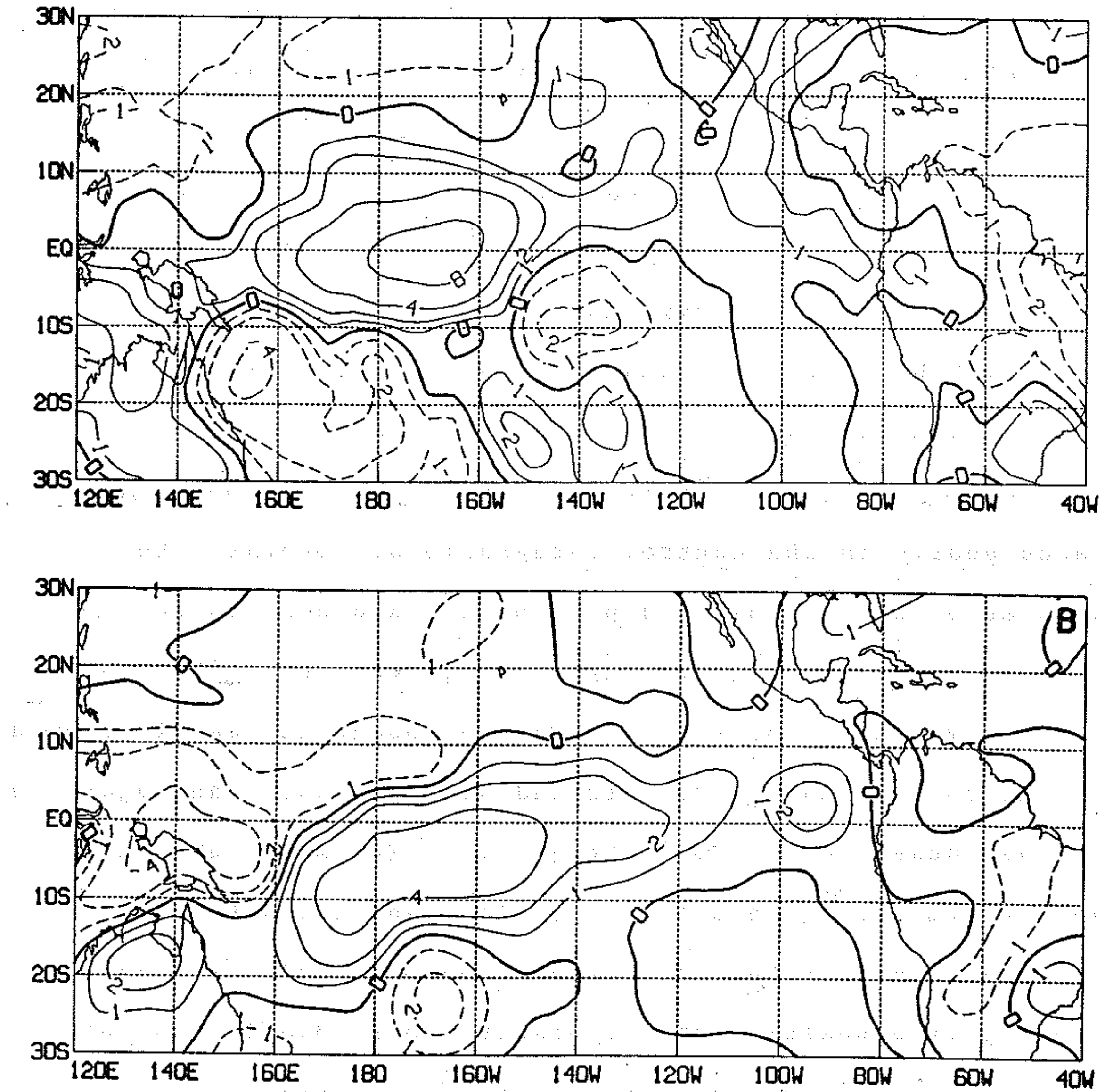

Fig. 3: 1-60 day 1987 mean precipitation for (a) observed anomaly calculated from observed OLR anomaly, and (b) simulated anomaly. Contours are 0, $\pm$ 1, 2, 4, 8, 12 mm day^{-1}. Dashed contours are negative.

central and eastern Pacific, with a maximum anomaly of over 12 mm/day in the vicinity of 150W (Fig. 2a). The positive anomaly in the simulated field greatly resembles that observed in both magnitude and position (Fig. 2b). The model also simulates the negative anomaly observed over Indonesia and Australia and the negative-positive anomaly dipole over Brazil. The main discrepancy is the models' failure to capture the observed extension of the positive anomaly to the SE, representing a shift in the SPCZ, which the model simulates poorly in the control integrations. Overall, the simulation of the observed precipitation anomalies in 1982-3 is very good. A large (4 mm/day) positive precipitation anomaly was also observed in 1987, although it was limited in extent to the central Pacific and did not reach the magnitude of that observed in 1982-3 (Fig. 3a). The model does a fair job of simulating this anomaly, although it positions it somewhat south of that observed. The model also simulates the negative-positive dipole observed over Brazil and the unusual positive anomaly over northern Australia. However, there is a very poor simulation of the main negative anomaly regions, with the model putting the main negative anomaly to the west of the large positive anomaly, while that observed was located south of the positive anomaly. Thus the 1987 simulated precipitation anomalies bear some resemblance to those observed, but not to the extent that the 1982-3 simulated anomalies did. Other tropical fields (sea level pressure, 850 mb winds, 200 mb winds) yield similar results, with well simulated features in both years, but stronger and better simulated anomalies in 1982-3 than in 1987 (not shown).

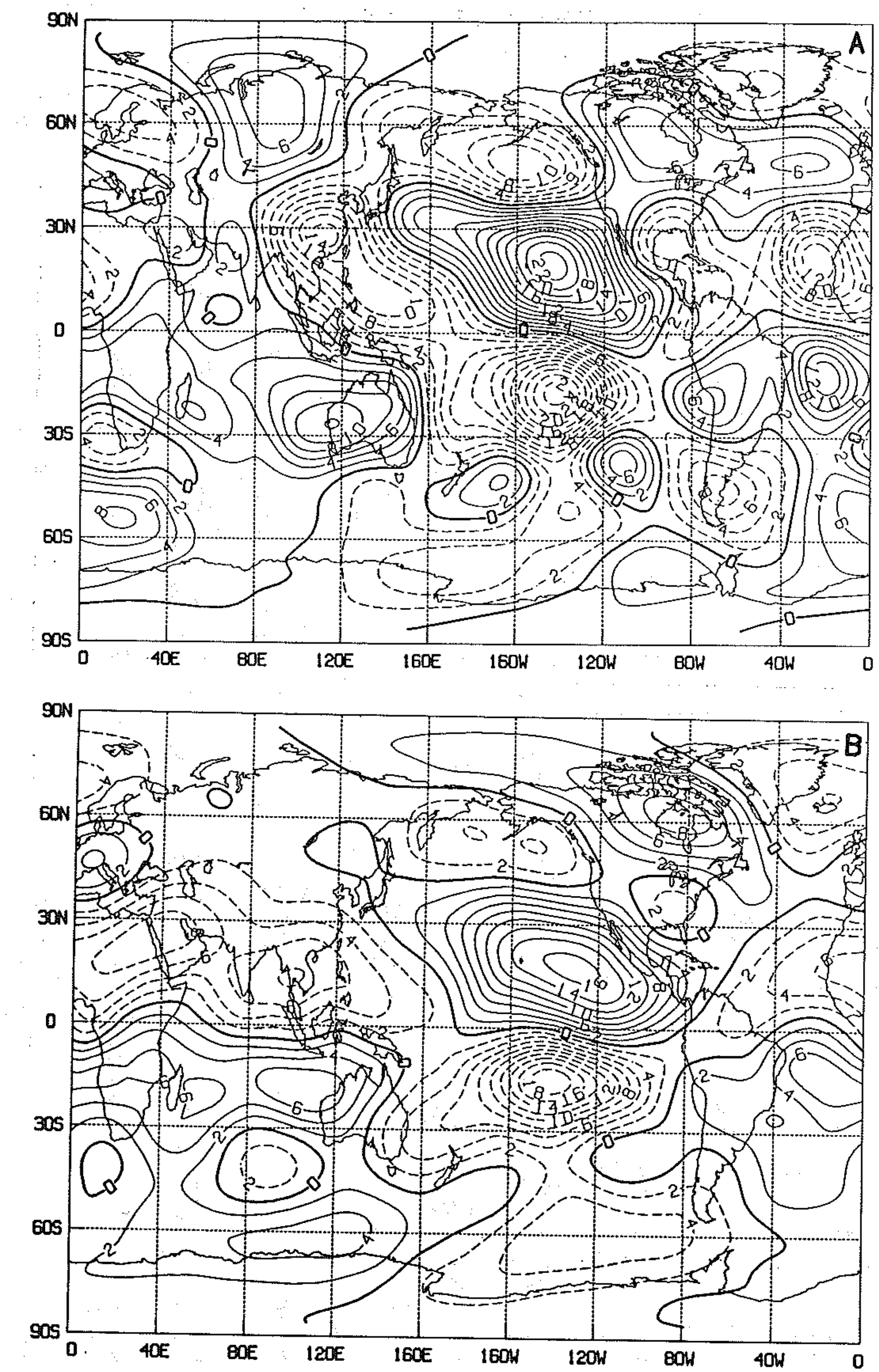

Fig. 4: 1-60 day 1982-3 mean zonal departure of 200 mb stream function for (a) observed anomaly from NMC analyses, and (b) simulated anomaly. Contour interval is $2 \times 10^6\ m^2 s^{-1}$. Dashed contours are negative.

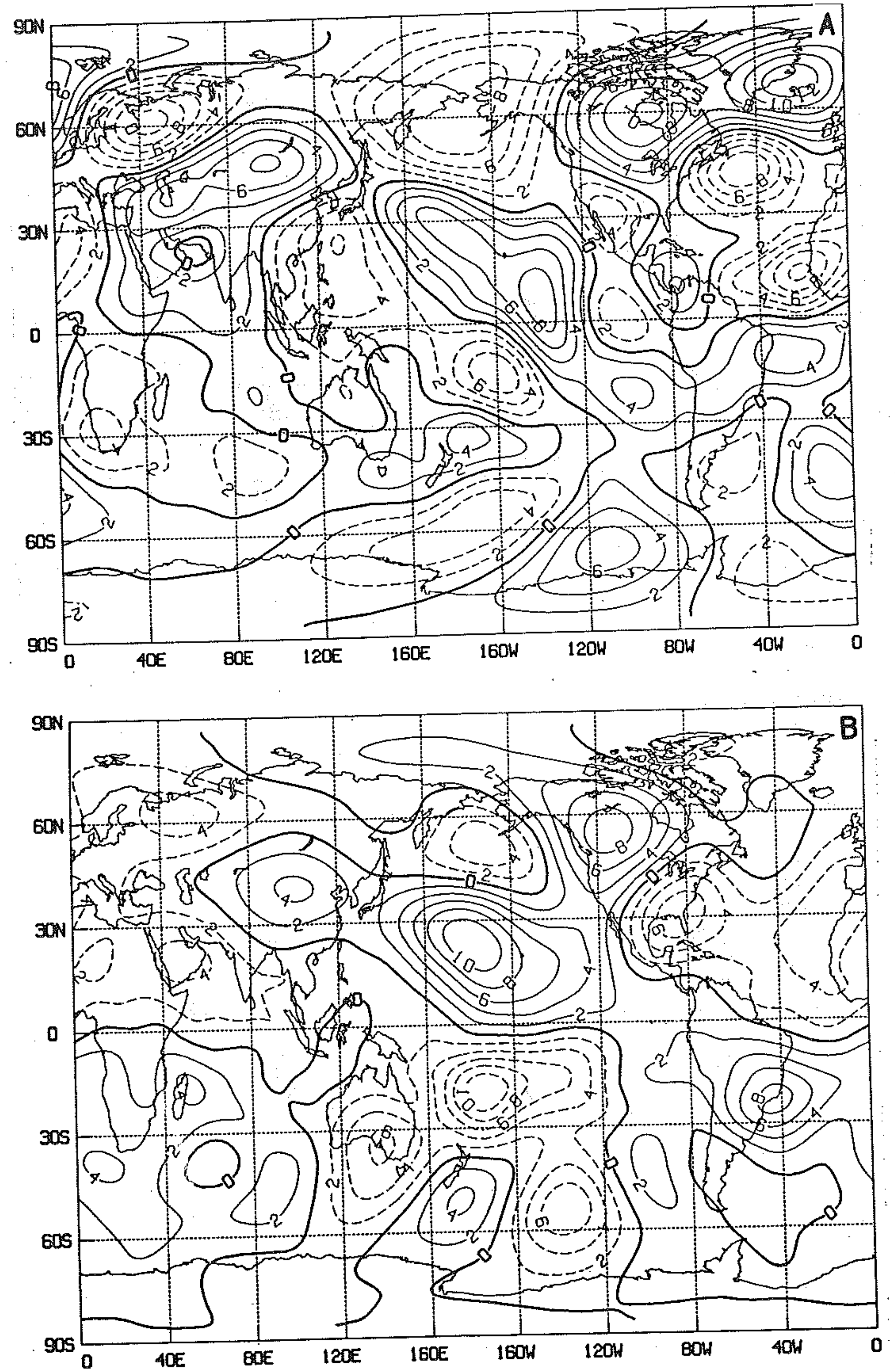

Fig. 5: 1-60 day 1987 mean zonal departure of 200 mb stream function for (a) observed anomaly from NMC analyses, and (b) simulated anomaly. Contour interval is $2 \times 10^6\ m^2 s^{-1}$. Dashed contours are negative.

The observed (from NMC analyses) and simulated anomalies in the zonal departure of 200 mb stream function for 1982-3 and 1987 are shown in Figs. 4 and 5 respectively. The observed anomaly for 1982-3 contains a strong anticyclonic couplet straddling the equator in the central and eastern Pacific and a weaker cyclonic couplet downstream in the tropics (Fig. 4a). These features are well simulated by the model, although their magnitude is a little weak (Fig. 4b). Over the Pacific and North America an eastward shifted PNA-like pattern (Wallace and Gutzler, 1981) is present in both the observed and simulated anomaly fields. In 1987 an anti-cyclonic couplet is also observed straddling the equator in the central Pacific, but it is smaller, weaker and westward of that observed in 1982-3 (Fig. 5a). The model correctly simulates this feature, although the position of the northern anticyclonic cell is somewhat south-east of that observed (Fig. 5b). The model also simulates the downstream cyclonic couplet observed in the tropics, which was also weaker than that in 1982-3. Over the Pacific and North America in 1987 a PNA like pattern somewhat similar to that in 1982-3 is observ-ed, although the 1987 pattern is not shifted as far eastward and the low over the Gulf of Mexico and Florida has been replaced by 2 lows to the east and west. In addition, a positive anomaly occurred in the vicinity of Greenland and Iceland instead of the negative anomaly observed in 1982-3. The model correctly simulates much of this 1987 pattern, but forecasts a single low over the Gulf of Mexico and Florida instead of the split low observed. Overall, the simulated 1987 extra-tropical features show some correspondence to those observed, but not as well as did the 1982-3 simulations. However, the observed and simulated extratropical features are of similar magnitude for the two years.

An overall picture of how the observed SST anomalies impacted the area mean forecasts can be seen in the 10 day mean RMS error of 300 mb geopotential (Fig. 6). The ensemble mean of the 3 control forecasts is shown as a dashed curve, while that for the 3 boundary forecasts is shown as a solid curve. In the tropics (20S-20N) a large increase in skill developed almost immediately in 1982-3, roughly halving the RMS error (Fig. 6a). In 1987, the tropical RMS error was also largely improved in the boundary simulations, although this improvement did not develop as quickly and was only half the magnitude of that in 1982-3. This slower development of the SST forecast improvement in 1987 vs. 1982-3 was also seen in 10- and 30-day time mean anomaly maps (not shown). The 1982-3 RMS error in the Northern Hemisphere (20N-76N) shows a modest foreast improvement by inclusion of the observed SST (Fig. 6c), however, this improvement was realized in each of the component members of the ensemble (not shown). In 1987, there was no forecast improvement in the first 20 days in the Northern Hemisphere followed by a modest improvement for the remainder of the experiment (Fig. 6d). This improvement in 1987 was not as reproducible as that in 1982-3, having occurred in only 2 of the 3 members of the ensemble. The 10-day mean time series of 300 mb geopotential anomaly correlation coefficient (not shown) reflects these same tropical and Northern Hemisphere features, as does the 30-day mean RMS

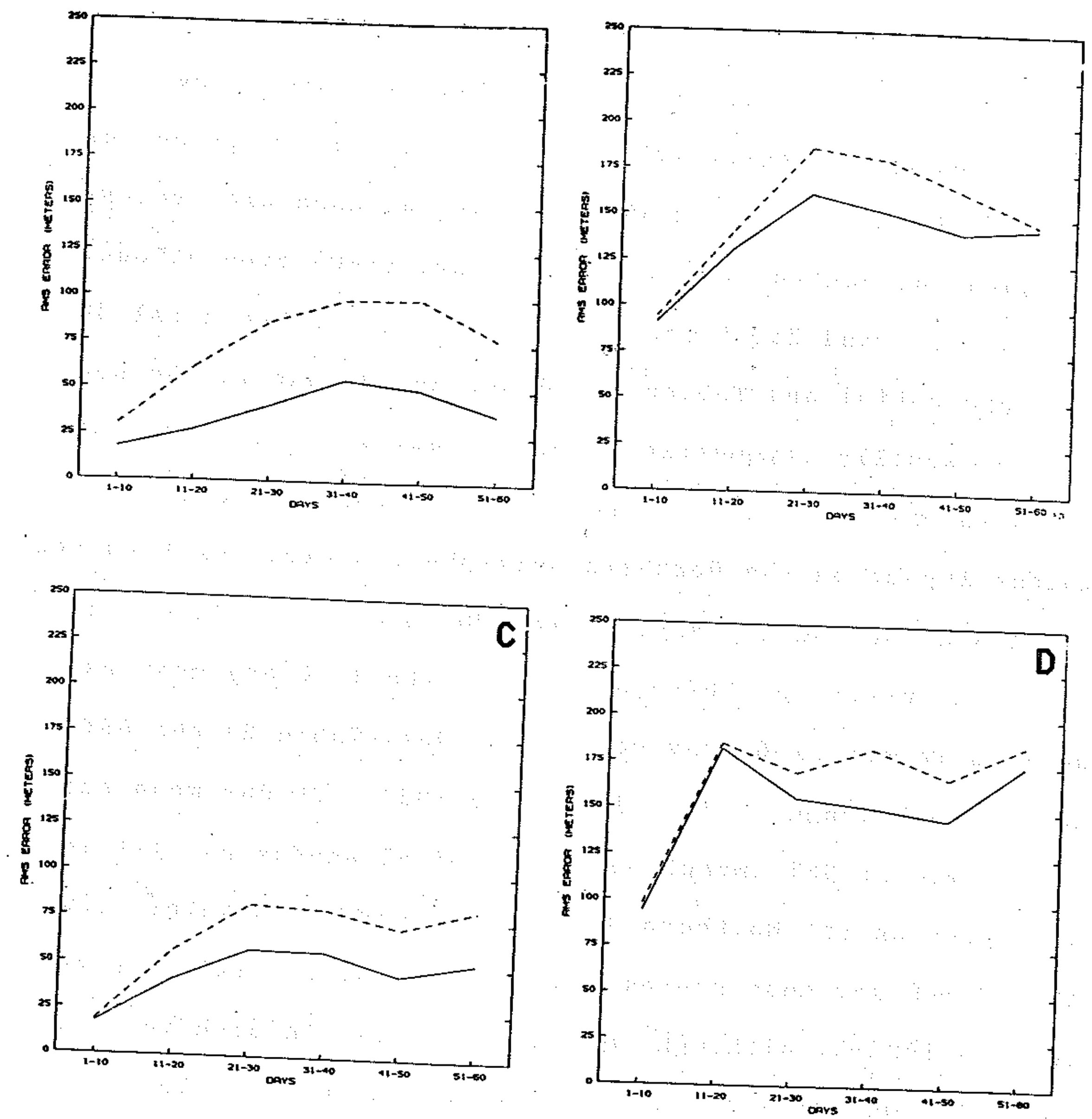

Fig. 6: 10-day mean RMS error of 300 mb geopotential (meters) for (a) 1982-3 tropics (20°S-20°N), (b) 1987 tropics, (c) 1982-3 Northern Hemisphere (20°N-76°N), and (d) 1987 Northern Hemisphere. Average of control integrations is dashed and average of the boundary integrations is solid.

error and anomaly correlation coefficient for 1982-3 (Table 1a, b) and 1987 (Table 2a, b). In Tables 1 and 2 the 30-day mean tropical and Northern Hemisphere scores are given for each initial condition as well as for the ensemble average for both the control (CON) and boundary (ANO) simulations. Tables 1a, b and 2a, b contain the scores for the total 300 mb geopotential and Tables 1c, d and 2c, d contain the scores for the zonally asymmetric component only. In 1982-3 (Table 1) there was a large SST impact on the tropical scores and a modest impact on the Northern Hemisphere scores for both the total and the zonally asymmetric 300 mb geopotential. This positive impact in 1982-3 occured in the 1-30 day mean as well as in the 31-60 day mean. In 1987 (Table 2) the SST impact took longer to develop. The 1987 1-30 day mean scores show a modest SST impact on the tropical scores and little or no impact on the Northern Hemisphere scores. However, the 1987 30-60 day mean scores display an impact similar to that seen in 1982-3, although somewhat weaker. In both years the control simulation total tropical anomaly correlation coefficients are negative, due to a negative model drift verifying against an observed positive tropical anomaly. It is interesting that in both years the positive SST impact on prediction is shared between the zonally symmetric and zonally asymmetric components of the flow.

4. DISCUSSION

Earlier studies have shown that the record 1982-3 El Niño Pacific SST anomalies were capable of producing a positive impact on prediction with a GCM in both the tropics and the

300MB GEOPOTENTIAL TOTAL RMS ERROR (M) **A**

I.C.	TROPICS (20S-20N) 1-30 CON	TROPICS 1-30 ANO	TROPICS 31-60 CON	TROPICS 31-60 ANO	NO. HEM. (20N-76N) 1-30 CON	NO. HEM. 1-30 ANO	NO. HEM. 31-60 CON	NO. HEM. 31-60 ANO
12/15/82	54	25	93	40	121	114	155	137
12/16/82	55	24	89	50	125	110	149	130
12/17/82	58	30	93	50	118	115	149	131
ENSEMBLE	58	27	91	46	122	112	138	120

300MB GEOPOTENTIAL TOTAL ANOMALY CORRELATION COEFFICIENT **B**

I.C.	TROPICS (20S-20N) 1-30 CON	TROPICS 1-30 ANO	TROPICS 31-60 CON	TROPICS 31-60 ANO	NO. HEM. (20N-76N) 1-30 CON	NO. HEM. 1-30 ANO	NO. HEM. 31-60 CON	NO. HEM. 31-60 ANO
12/15/82	-0.53	0.75	-0.75	0.56	0.15	0.19	0.18	0.42
12/16/82	-0.53	0.76	-0.69	0.21	-0.05	0.24	0.37	0.43
12/17/82	-0.53	0.61	-0.76	0.23	0.06	0.24	0.41	0.48
ENSEMBLE	-0.60	0.71	-0.75	0.35	0.00	0.18	0.36	0.49

300MB GEOPOTENTIAL ZONALLY ASYMMETRIC RMS ERROR (M) **C**

I.C.	TROPICS (20S-20N) 1-30 CON	TROPICS 1-30 ANO	TROPICS 31-60 CON	TROPICS 31-60 ANO	NO. HEM. (20N-76N) 1-30 CON	NO. HEM. 1-30 ANO	NO. HEM. 31-60 CON	NO. HEM. 31-60 ANO
12/15/82	20	13	33	19	84	81	116	97
12/16/82	19	16	29	22	70	58	97	88
12/17/82	21	14	36	17	74	77	106	91
ENSEMBLE	20	13	32	18	73	67	90	78

300MB GEOPOTENTIAL ZONALLY ASYMMETRIC ANOMALY CORR. COEFF. **D**

I.C.	TROPICS (20S-20N) 1-30 CON	TROPICS 1-30 ANO	TROPICS 31-60 CON	TROPICS 31-60 ANO	NO. HEM. (20N-76N) 1-30 CON	NO. HEM. 1-30 ANO	NO. HEM. 31-60 CON	NO. HEM. 31-60 ANO
12/15/82	0.20	0.72	-0.29	0.69	0.19	0.28	-0.04	0.41
12/16/82	0.32	0.60	0.05	0.59	0.25	0.61	0.32	0.43
12/17/82	0.24	0.71	-0.37	0.73	0.27	0.39	0.35	0.47
ENSEMBLE	0.20	0.69	-0.24	0.70	0.18	0.42	0.31	0.53

Table 1: 1982-3 30-day mean tropics and Northern Hemisphere 300 mb geopotential (a) total RMS error, (b) total anomaly correlation coefficient, (c) zonally asymmetric RMS error and (d) zonally asymmetric anomaly correlation coefficient.

300MB GEOPOTENTIAL TOTAL RMS ERROR (M) **A**

I.C.	TROPICS (20S-20N) 1-30 CON	TROPICS 1-30 ANO	TROPICS 31-60 CON	TROPICS 31-60 ANO	NO. HEM. (20N-76N) 1-30 CON	NO. HEM. 1-30 ANO	NO. HEM. 31-60 CON	NO. HEM. 31-60 ANO
1/1/87	44	29	78	46	124	117	155	122
1/2/87	43	31	71	53	124	126	154	144
1/3/87	49	34	80	52	126	131	142	135
ENSEMBLE	49	33	76	50	124	122	144	125

300MB GEOPOTENTIAL TOTAL ANOMALY CORRELATION COEFFICIENT **B**

I.C.	TROPICS (20S-20N) 1-30 CON	TROPICS 1-30 ANO	TROPICS 31-60 CON	TROPICS 31-60 ANO	NO. HEM. (20N-76N) 1-30 CON	NO. HEM. 1-30 ANO	NO. HEM. 31-60 CON	NO. HEM. 31-60 ANO
1/1/87	-0.47	0.29	-0.74	-0.28	0.24	0.32	0.16	0.45
1/2/87	-0.43	0.20	-0.73	-0.48	0.25	0.26	0.23	0.39
1/3/87	-0.57	0.07	-0.75	-0.35	0.18	0.21	0.37	0.26
ENSEMBLE	-0.58	0.04	-0.75	-0.38	0.21	0.26	0.24	0.36

300MB GEOPOTENTIAL ZONALLY ASYMMETRIC RMS ERROR (M) **C**

I.C.	TROPICS (20S-20N) 1-30 CON	TROPICS 1-30 ANO	TROPICS 31-60 CON	TROPICS 31-60 ANO	NO. HEM. (20N-76N) 1-30 CON	NO. HEM. 1-30 ANO	NO. HEM. 31-60 CON	NO. HEM. 31-60 ANO
1/1/87	19	17	22	19	92	90	98	76
1/2/87	19	16	21	22	87	90	90	97
1/3/87	19	17	21	21	76	85	93	83
ENSEMBLE	19	16	20	19	83	83	84	72

300MB GEOPOTENTIAL ZONALLY ASYMMETRIC ANOMALY CORR. COEFF. **D**

I.C.	TROPICS (20S-20N) 1-30 CON	TROPICS 1-30 ANO	TROPICS 31-60 CON	TROPICS 31-60 ANO	NO. HEM. (20N-76N) 1-30 CON	NO. HEM. 1-30 ANO	NO. HEM. 31-60 CON	NO. HEM. 31-60 ANO
1/1/87	0.12	0.18	0.05	0.29	0.31	0.38	0.27	0.62
1/2/87	0.14	0.26	-0.05	0.10	0.34	0.37	0.40	0.54
1/3/87	0.14	0.20	0.04	0.27	0.32	0.32	0.56	0.44
ENSEMBLE	0.14	0.22	0.00	0.24	0.32	0.37	0.45	0.58

Table 2: 1987 30-day mean tropics and Northern Hemisphere 300 mb geopotential (a) total RMS error, (b) total anomaly correlation coefficient, (c) zonally asymmetric RMS error and (d) zonally asymmetric anomaly correlation coefficient.

extra-tropics. Results from simulations with the 1986-7 El Niño Pacific SST anomalies show that a positive impact on prediction can occur even when the SST anomalies are of more typical magnitude. This finding is encouraging due to the relatively frequent occurrence of moderate El Niño SST anomalies and the prospect of predicting them with a coupled atmosphere-ocean model.

Although a positive forecast impact was obtained by including the Pacific SST anomalies from both of these 2 years, important differences in this impact are seen by comparing the two. The observed and simulated time mean anomalies in the tropics were much larger in 1982-3 than in 1987. The impact of including the observed SST anomalies on the forecast skill scores in the tropics was also much larger in 1982-3. Thus, the impact of the observed SST anomalies on prediction in the tropics does seem related to the strength of the SST anomalies. In 1982-3 the SST anomalies were large enough to extend the region of very warm (~29°) water normally confined to the western equatorial Pacific, across the entire equatorial Pacific basin. In 1987, as in the composite case of Rasmusson and Carpenter (1982), the SST anomalies merely extend this very warm water a little eastward into the central Pacific. This region where the very warm equatorial water has been extended is where the major anomalous convection and heating occur in both the observations and the GCM. Thus, this region of anomalous heating is much larger in 1982-3 than in 1987 and the tropical forecast impact is much larger. The strength of the SST anomalies also seems to affect the response time of the GCM, with a positive forecast impact developing more rapidly in 1982-3 than in 1987 in both the tropics and extra-tropics.

The forecast impact in the extra-tropics does not seem to be very well related to the strength of the SST anomalies or even the strength and expanse of the tropical heating and divergence anomalies. A modest forecast improvement occurred in the extra-tropics in both 1982-3 and 1987, slightly more in 1982-3. The time mean simulated anomalies also resembled their observed counterparts somewhat better in 1982-3 than in 1987. However, it is interesting that the observed and simulated extra-tropical anomalies were of similar magnitude in the two years, whereas the tropical anomalies were much larger in 1982-3. This suggests that the extra-tropical anomalies may not be directly forced by the tropical heating and divergence anomalies. Recent studies by Held and Kang (1987) and Sardeshmukh and Hoskins (1988) using barotropic models show that forcing from the sub-tropics may be more important than that from the tropics in evoking an extra-tropical response. Following their example, the authors calculated the complete time mean anomalous Rossby wave source for these two years. In both the observations and the simulations the largest signals were in the sub-tropics, not the tropics. This anomalous Rossby wave source was of similar magnitude for the two years, although the pattern, which was fairly well simulated in each year, was quite different between the two. The similar strength of this subtropical forcing is a possible explanation for the similar magnitude

of the extra-tropical anomalies in these two years, although further work is required on this subject.

5. ACKNOWLEDGEMENTS

The authors would like to thank Ms. Diane C. Marsico of CAC for providing the SST anomalies used in this study. We are grateful to Ms. Marlene Schllichtig for her careful preparation of the manuscript. Finally, we would like to thank Dr. S. Nigam for enlightening discussions on some of the calculations presented.

6. REFERENCES

Arakawa, A., 1969: Parameterization of cumulus convection, Proc. WMO/IUGG Symp. on Numerical Prediction, Tokyo, 1-6.

Deardorff, J. W., 1972: Parameterization of the planetary boundary layer for use in general circulation models. Mon. Wea. Rev., 100, 93-106.

Fennessy, M. J., L. Marx and J. Shukla, 1985: General Circulation model sensitivity to 1982-83 equatorial Pacific sea surface temperature anomalies. Mon. Wea. Rev., 113, 858-864.

Fennessy, M. J. and J. Shukla, 1988: Numerical simulation of the atmospheric response to the time-varying El Niño SST anomalies during May 1982 through October 1983. J. Climate, 1, 195-211.

Held, I. M. and I.S. Kang, 1987: Barotropic models of the extratropical response to El Nino, J. Atmos. Sci., 44, 3576-3586.

Owen, J. A. and T. N. Palmer, 1987: The impact of El Nino on an ensemble of extended-range forecasts. Mon. Wea. Rev., 115, 2103-2117.

Randall, D. A., 1976: The interaction of the planetary layer with large-scale circulations. Ph.D. thesis, UCLA, 247 pp.

Rasmusson, E. M. and T. H. Carpenter, 1982: Variations in the tropical sea surface temperature and surface wind fields associated with the Southern Oscillation/El Niño. Mon. Wea. Rev., 110, 354-384.

Sardeshmukh, P. D. and B. J. Hoskins, 1988: Generation of global rotational flow by steady idealized tropical divergence. J. Atmos. Sci., 45, 1228-1251.

Shukla, J. and M. J. Fennessy, 1988: Prediction of time mean atmospheric circulation and rainfall: Influence of Pacific SST anomaly. J. Atmos. Sci., 45, 9-28.

Tokioka, T., K. Yamazaki and M. Chiba, 1987: A case study of the impact of sea-surface temperature anomalies and initial conditions on dynamical forecast up to two months in the early summer of 1983. Papers in Met. and Geophysics, 38, 265-277.

Wallace, J. M. and D. S. Gutzler, 1981: Teleconnections in the geopotential height field during the Northern Hemisphere winter. Mon. Wea. Rev., 109, 784-812.

WMO, 1986: Workshop on comparison of simulations by numerical models of the sensitivity of the atmospheric circulation to sea surface temperature anomalies. WMO/TD-No. 138, WCP-121, World Meteorological Organization, Geneva, pp. 188.